

Neutral copper(I) phosphorescent complexes from their ionic counterparts with 2-(2'-quinoly)benzimidazole and phosphine mixed ligands†

Junhui Min,^{a,c} Qisheng Zhang,^b Wei Sun,^{a,c} Yanxiang Cheng^{*a,b} and Lixiang Wang^{*a}

Received 17th August 2010, Accepted 26th October 2010

DOI: 10.1039/c0dt01031f

Neutral mononuclear Cu^I complexes and their counterparts with counterion, *i.e.* Cu(qbm)(PPh₃)₂, Cu(qbm)(DPEphos), [Cu(Hqbm)(PPh₃)₂](BF₄) and [Cu(Hqbm)(DPEphos)](BF₄), where Hqbm = 2-(2'-quinoly)benzimidazole, DPEphos = bis[2-(diphenylphosphino)phenyl]ether, have been synthesized and characterized by X-ray structure analyses. All of the four complexes in solid state exhibit a strong phosphorescence band in the orange spectral region at room temperature. The photophysical properties of these complexes in both methylene chloride solution and poly(methyl methacrylate) film have been studied. Compared to the related cationic complexes, the neutral ones show blue-shifted emissions and longer lifetimes that can be attributed to the additional ligand-centered $\pi-\pi^*$ transition beside traditional metal-to-ligand charge-transfer (MLCT). By doping these complexes in *N*-(4-(carbazol-9-yl)phenyl)-3,6-bis(carbazol-9-yl) carbazole (TCCz), multilayer organic light-emitting diodes (OLEDs) were fabricated with the device structure of ITO/PEDOT/TCCz: Cu^I (10 wt%)/BCP/Alq₃/LiF/Al. The neutral complex Cu(qbm)(DPEphos) exhibits a higher current efficiency, up to 8.87 cd A⁻¹, than that (5.58 cd A⁻¹) of its counterpart [Cu(Hqbm)(DPEphos)](BF₄).

Introduction

Photoluminescent Cu^I complexes based on α,α' -diimine and triphenylphosphine mixed ligand have attracted much attention recently because of their highly phosphorescence from metal-to-ligand charge-transfer (MLCT) excited state and possible utilization in electroluminescent devices,¹ for which they exhibit remarkable performance with the external quantum efficiency comparable to those third-row noble Ir^{III}, Pt^{II}, and Os^{II} complexes.² However, these cationic Cu^I emitters suffer two disadvantages of the device fabrication. First, most of these mixed-ligand Cu^I complexes exhibit poor volatility due to their ionic nature and can't fabricate the small-molecule organic light-emitting diodes (OLEDs) by the conventional vacuum deposition method, which always achieve more excellent device performance than those polymer light-emitting diodes (PLEDs) fabricated by spin-coating. Second, it is generally recognized that the small counterions of ionic complex presented in the luminescent layer would decrease the performance of the device by affecting the balance of charges

injection.³ Similar phenomenon has also been found in the OLEDs based on ionic Cu^I complexes.⁴ Therefore, the charge-neutral Cu^I phosphorescent complexes without counterions have been expected to improve the performance of the OLEDs device.

Recently, several research groups have undertaken the photophysical study of neutral mononuclear, dinuclear and trinuclear Cu^I complexes supported by individual bidentate, tridentate and mixed ligands. For example, Omary *et al.* reported that a neutral trinuclear Cu^I complex with fluorinated pyrazolate ligands exhibits multicolor bright phosphorescent emissions that are sensitive to temperature, solvent and concentration.⁵ More recently, Peter *et al.* reported an example of neutral dinuclear Cu^I complex, [Cu(PNP-^tBu)]₂, using tridentate PNP ligand ([PNP]⁻ = bis(2-(diisobutylphosphino)phenyl)amide), which exhibits excellent quantum yield even in polar solvents due to a strongly rigid structure resulting from steric hindrance of the ligand and the absence of a counterion,⁶ and a kind of neutral mononuclear Cu^I complex supported by amidophosphine ligands with quantum efficiency in the range of 0.16–0.70 and lifetimes as long as 150 μ s in benzene solution.⁷ More exciting, the maximum external quantum efficiencies (EQE) of 16.1% has been reported by using the above complex, [Cu(PNP-^tBu)]₂, while submitting our manuscript.^{6b} However, neutral Cu^I complexes still remain rare compared to a great deal of cationic Cu^I compounds.

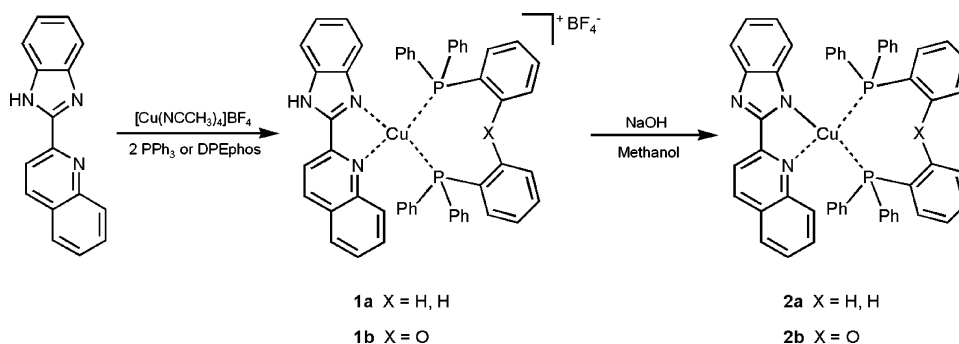
In this paper, we report two pairs of mononuclear diimine/diphosphine mixed-ligand Cu^I complexes with (ionic form) and without counterions (neutral form), which possess completely identical skeletons but quite different photophysical properties in each pair. The first ligand used in this study, as a key factor, is

^aState Key Laboratory of Polymer Physics and Chemistry, Changchun Institute of Applied Chemistry, Chinese Academy of Science, Changchun, 130022, P. R. China. E-mail: yanxiang@ciac.jl.cn, lixiang@ciac.jl.cn; Fax: 86-431-85684937; Tel: +86-431-85262106

^bState Key Laboratory of Structural Chemistry, Fujian Institute of Research on the Structure of Matter, Chinese Academy of Sciences, Fuzhou, 350002, P. R. China

^cThe Graduate School, Chinese Academy of Sciences, Beijing, 100039, P. R. China

† CCDC reference numbers 724902–724905. For crystallographic data in CIF or other electronic format see DOI: 10.1039/c0dt01031f



Scheme 1 The synthesis route of mononuclear copper(I) complexes.

2-(2'-quinolyl)benzimidazole (Hqbm), which can offer two kinds of coordination features. One is from two sp^2 N atoms located in quinolyl and benzimidazole ring, respectively, to form the cationic Cu^I complexes. Another is from a sp^2 N atom in a quinolyl ring and a sp^3 N atom of NH group in a benzimidazole ring to prepare neutral complexes by removing the active H atom in the presence of a strong base.

Results and discussion

Synthesis and characterization

The synthesis of neutral qbm Cu^I complex with triphenylphosphine (PPh_3) or bis[2-(diphenylphosphino)phenyl]ether (DPEphos) as the second ligand *via* a two step reaction is outlined in Scheme 1. Reaction of $[Cu(NCCH_3)_4](BF_4)$ with Hqbm and phosphine ligands gives ionic complex $[Cu(Hqbm)(PPh_3)_2](BF_4)$ (**1a**) and $[Cu(Hqbm)(DPEphos)](BF_4)$ (**1b**) in high yield first. By treating **1a** or **1b** with NaOH mixture in methanol, the neutral $Cu(qbm)(PPh_3)_2$ (**2a**) or $Cu(qbm)(DPEphos)$ (**2b**) can be subsequently isolated in 80 and 59% yield by recrystallization in chloroform–methanol, respectively. All of the Cu^I complexes are stable in air and characterized by 1H and ^{31}P NMR spectra, in which both **1a** and **1b** show the proton signals of imidazole rings at about 12 ppm, and ^{31}P signals (about -1.0 ppm for **1a** and **2a**, about -12 ppm for **1b** and **2b**) shift down field compared with those of free phosphine ligands (-4.60 for PPh_3 and -16.40 for DPEphos).

Neutral complexes can simply convert back into ionic complexes while adding light excess 40% HBF_4 solution, monitored by 1H NMR. The pK_a values measured by UV-visible spectrometry are 9.47 and 9.11 for complexes **1a** and **1b**, respectively, while the free ligand, Hqbm, shows no shift in its spectrum under the same conditions. However, the longer-wavelength peak red-shifts from 333 to 356 nm in the methanol of KOH instead of 6 : 4 methanol–water solution, indicating the pK_a value of the free ligand is bigger than that of water. The smaller pK_a of the complexes, relative to the free ligand, indicates that the coordination decreases the acidity of the proton on the imidazole ring.

The molecular structures of four Cu^I complexes have been determined by X-ray diffraction. Fig. 1–4 show the perspective drawing of all complexes and Table 1 lists selected bond distances and bond angles. Although all complexes exhibit similar distorted tetrahedral coordination geometries, several differences stem from the loss of the counterion and active H. First, the $Cu-N$ distances

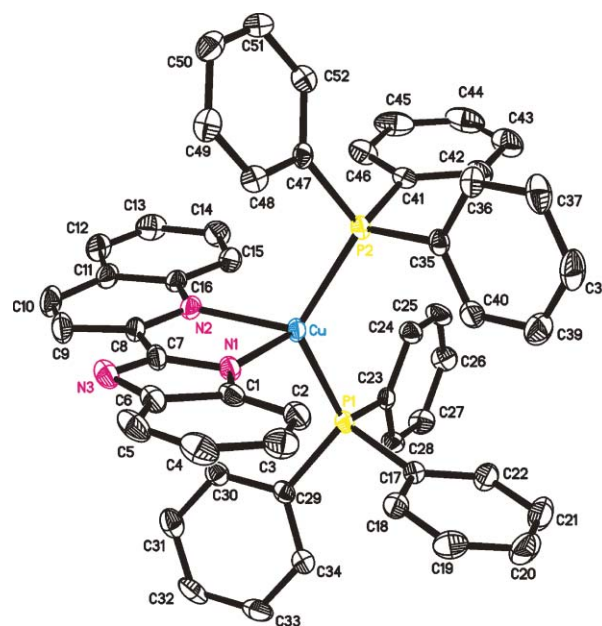


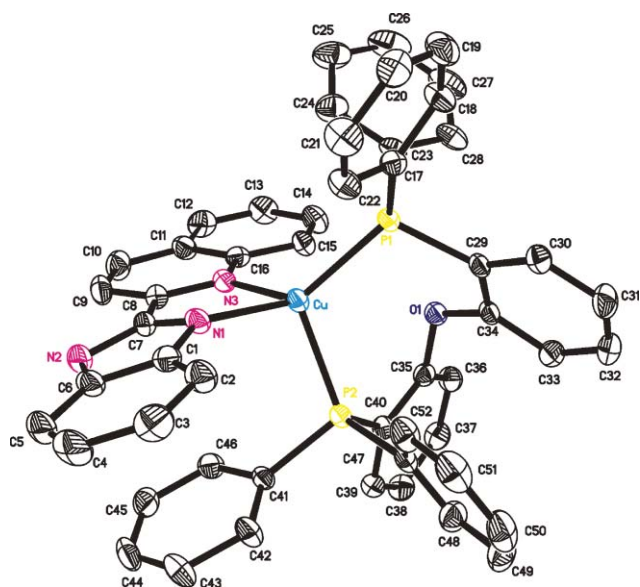
Fig. 1 ORTEP representation of the structure of the cation in $[Cu(qbm)(PPh_3)_2](BF_4) \cdot 2CH_2Cl_2$ (**1a**). Thermal ellipsoids are drawn at the 30% probability level. Solvent molecules, the anion and H atoms are omitted for clarity.

of neutral Cu^I complexes shorten due to the stronger bonding ability of negatively charged benzimidazole. For example; the $Cu-N$ distances of 2.064 and 2.118 Å in neutral complex **2a** are obviously shorter than those of 2.087 and 2.133 Å in **1a**, while the $Cu-P$ distances are similar both in **1a** and **2a**. Second, the negative charge on benzimidazole ring reshapes the five-membered rings dramatically and the bond distances of $C-N$ in imidazole rings tend to average for neutral Cu^I complexes. Third, the torsion angles $N1-C7-C8-N2$ of **1a** and **1b** (8.25 and 4.35°) are obviously reduced relative to **2a** and **2b** (9.12 and 11.34°). The latter two facts reveal that there is a stronger aromaticity on the NN chelating ligand of neutral Cu^I complexes.

Another structural character is the existence of intramolecular $\pi-\pi$ interactions between benzimidazolyl and phenyl rings with 3.391 Å of $C41-N1$ in **1b** and 3.642 Å of $C42-N1$ in **2b**, respectively, while DPEphos as the second ligand. The similar feature was observed in the compound $[Cu(phen)(dppf)](BF_4)$, [where $dppf = 1,1'$ -bis(diphenylphosphino)ferrocene],⁸ due to the restricted bite angle of the bidentate ligand, which always results in the more

Table 1 Selected bond distances (Å) and bond angles (°) for all complexes

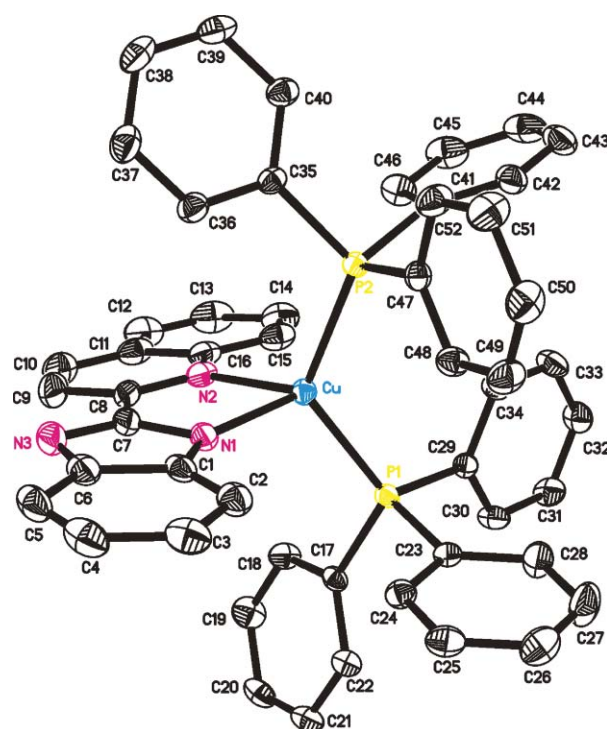
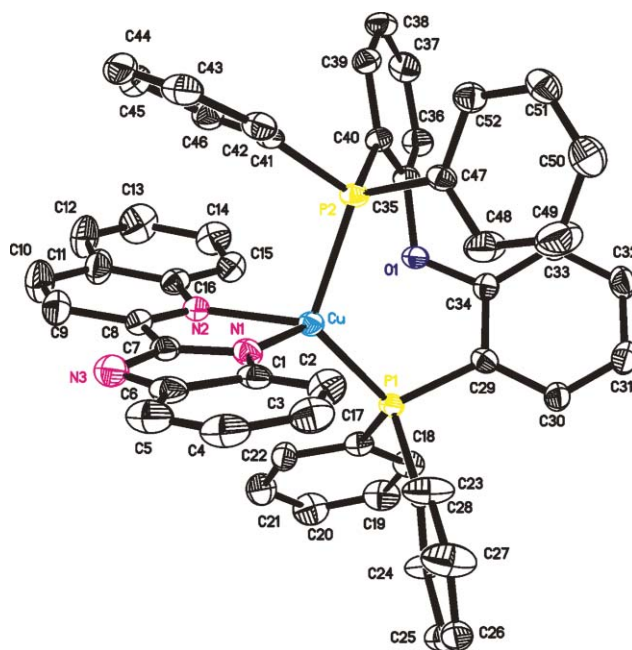
Complexes	1a	1b	2a	2b
Cu–N1	2.087 (3)	2.074 (3)	2.064 (2)	2.048 (5)
Cu–N2	2.133 (3)	2.122 (3)	2.118 (2)	2.086 (5)
Cu–P1	2.2633 (10)	2.2915 (11)	2.2630 (7)	2.2223 (15)
Cu–P2	2.2676 (10)	2.2227 (11)	2.2757 (8)	2.2741 (15)
N1–C1	1.393 (4)	1.399 (5)	1.382 (4)	1.424 (8)
N1–C7	1.332 (4)	1.317 (5)	1.343 (4)	1.344 (8)
C7–C8	1.455 (5)	1.455 (6)	1.441(5)	1.434 (9)
N3–C7	1.374 (4)	1.382 (5)	1.356 (4)	1.359 (7)
N3–C6	1.391 (4)	1.372 (5)	1.372 (4)	1.410 (9)
C6–C1	1.407 (4)	1.406 (6)	1.416 (4)	1.409 (9)
N2–C8	1.324 (4)	1.342 (5)	1.345 (4)	1.338 (8)
N1–Cu–N2	79.31 (11)	80.50 (12)	80.76 (10)	81.0 (2)
P1–Cu–P2	124.24 (3)	112.40 (4)	124.00 (3)	117.08 (6)
N1–Cu–P1	111.23 (8)	101.71 (9)	113.16 (7)	124.01 (14)
N1–Cu–P2	109.49 (8)	130.56 (10)	107.59 (7)	104.65 (13)
N2–Cu–P1	109.97 (8)	106.65 (9)	109.88 (7)	120.36 (14)
N2–Cu–P2	113.68 (8)	119.71 (9)	113.21 (7)	103.02 (13)
N1–C7–C8–N2	9.12	11.34	8.25	4.35

**Fig. 2** ORTEP representation of the structure of the cation in [Cu(qbm)(POP)](BF₄)·1.5CH₃OH·1.5CH₂Cl₂·1.5H₂O (**1b**). Thermal ellipsoids are drawn at the 30% probability level. Solvent molecules, the anion and H atoms are omitted for clarity.

distorted tetrahedral geometries in Cu^I complexes. In contrast, there is no intramolecular π – π interaction in **1a** and **2a**, and their coordination geometries tend towards an ideal tetrahedron. In addition, compounds **1a**, **2a** and **1b** display intermolecular π – π interactions between the quinolyl rings of two adjacent molecules with 3.417 (C6A–C6B), 3.574 (C11A–C11B) and 3.495 Å (C11A–C13B, Fig. 5), respectively.

Photophysical and electrochemical properties

The absorption and emission spectra for four Cu^I complexes in CH₂Cl₂ are shown in Fig. 6. All complexes display an intense π – π^* transition centered on 2-(2'-quinolyl)benzimidazolyl at 359 and 355 nm for **1a** and **1b**, 387 and 383 nm for **2a** and **2b**, respectively. The red shift of the π – π^* absorption of the neutral

**Fig. 3** ORTEP representation of the structure of Cu(qbm)(PPh₃)₂·2CH₃OH (**2a**). Thermal ellipsoids are drawn at the 30% probability level. Solvent molecules and H atoms are omitted for clarity.**Fig. 4** ORTEP representation of the structure of Cu(qbm)(POP)·CH₃OH (**2b**). Thermal ellipsoids are drawn at the 30% probability level. Solvent molecule and H atoms are omitted for clarity.

complexes is not surprising in comparison to that of cationic forms, which is consistent with the stronger conjugation ligands in the neutral complexes after the removal of proton from 2-(2'-quinolyl)benzimidazole. The characteristic MLCT absorption bands ($\epsilon \approx 3000 \text{ M}^{-1} \text{ cm}^{-1}$) can be observed clearly in cationic

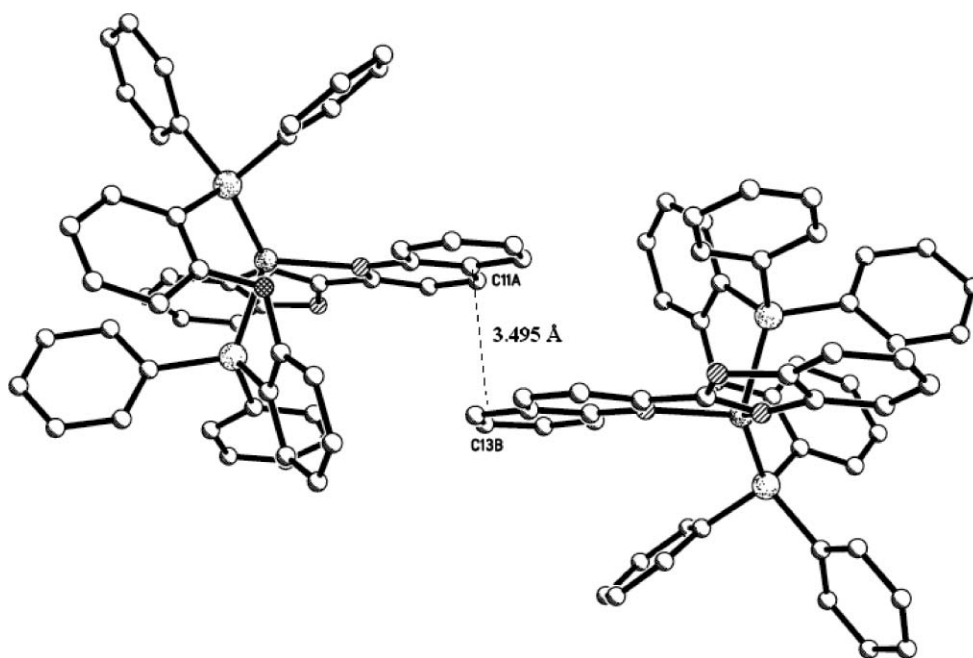


Fig. 5 Crystal packing diagram between adjacent molecules of the cation in $[\text{Cu}(\text{qbm})(\text{POP})](\text{BF}_4) \cdot 1.5\text{CH}_3\text{OH} \cdot 1.5\text{CH}_2\text{Cl}_2 \cdot 1.5\text{H}_2\text{O}$ (**1b**). Solvent molecules, the anion and H atoms are omitted for clarity.

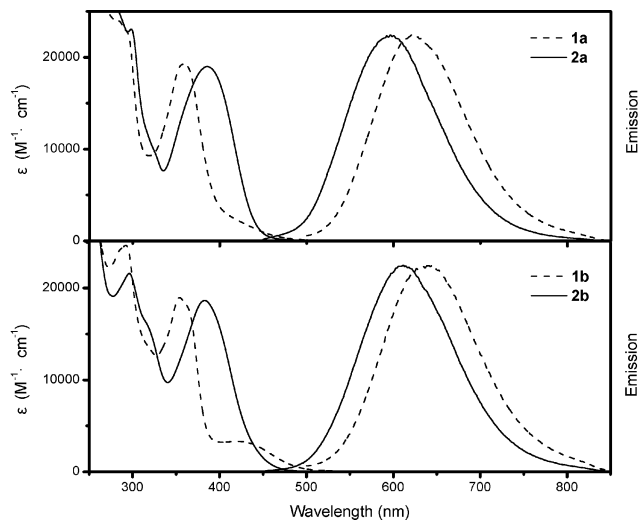


Fig. 6 The absorption (left) and emission spectra (right) of four Cu^{I} complexes in CH_2Cl_2 at room temperature.

complexes **1a** and **1b** at 415 and 425 nm, respectively, when these, even as the shoulder in neutral **2a** and **2b** disappear along with red shift of $\pi-\pi^*$ bands. The emission spectra of the four complexes show a broad orange-red emission band in DCM at room temperature. The emission spectra of neutral complexes show λ_{max} at 596 nm for **2a** and 612 nm for **2b**, both of which blue-shift 26 nm compared to their parent cationic complexes **1a** and **1b**.

The quantum efficiency and lifetime of each complex in degassed DCM varies widely depending on the auxiliary ligand as well as the electronegativity of NN ligand, as listed in Table 2. For the cationic complexes based on Hqbm, PPh_3 complex (**1a**) exhibits a 2-fold greater quantum efficiency and lifetime

than DPEphos (**1b**), quite like the similar 2,2'-biquinoline (bq) complexes reported previously. What's more, the radiative decay rate ($k_r = \phi / \tau$) of these two complexes is about $3.7\text{--}3.9 \times 10^3 \text{ s}^{-1}$, also very close to the value of bq complexes ($3.6 \times 10^3 \text{ s}^{-1}$ for $[\text{Cu}(\text{bq})(\text{PPh}_3)_2]^+$ and $3.3 \times 10^3 \text{ s}^{-1}$ for $[\text{Cu}(\text{bq})(\text{DPEphos})]^+$) due to the close NN ligand structures.^{2c} Comparing the neutral complexes to their parent cationic complexes, the quantum efficiency of **2b** ($\phi = 0.015$) is much higher than that of **1b** ($\phi = 0.0020$), while that of **2a** ($\phi = 0.0035$) is slightly lower than that of **1a** ($\phi = 0.0042$). Ignoring the difference in emission efficiency, the lifetimes of the neutral complexes are both several times longer than their parent cationic ones.

The solid of four Cu^{I} complexes display bright yellow-orange luminescence under a hand-held UV lamp. Their photophysical data in poly(methyl methacrylate) (PMMA) film (20 wt% in PMMA) were also studied (Table 2). The absorption spectra of four Cu^{I} complexes in solid film are similar to those in DCM, while their emission spectra blue shift 40–60 nm. In addition, both quantum yield and lifetime significantly increased in polymer films because the rigid medium can sterically prevent the excited-state distortion of phosphorescent heavy metal complexes and therefore decrease the non-radiative decay, as previously reported in Ru^{II} ,⁹ Ir^{III} ,¹⁰ and Cu^{I} systems.^{2a,2c,11} As in solution, the emission spectra blue-shift and the lifetimes have almost doubled when comparing the neutral complexes with their parent cationic complexes. However, the quantum efficiencies of all complexes in solid film are very close within the range of 0.12–0.16.

With reference to previous work,^{12,13} it can be deduced that the lowest excited state of the cationic complexes **1a** and **1b** is principally attributed to the MLCT state. However, the case in the neutral complexes **2a** and **2b** are more complicated. First, the emissive excited state of the neutral complexes still has MLCT character, because their photophysical characteristic

Table 2 Photophysical and electrochemical data for Cu^I complexes at room temperature

Compound	Absorption in DCM		Emission in DCM			Emission in 20 wt% PMMA film			$\Delta E^d/eV$	HOMO ^e /LUMO ^f /eV
	λ_{max}/nm ($\epsilon/M^{-1}cm^{-1}$)	λ_{max}/nm	ϕ^a	$\tau^b/\mu s$	λ_{max}/nm	ϕ^a	$\tau^c/\mu s$			
1a	359 (19 263), 415 (2522)	622	0.0042	1.09	570	0.14	26.8	2.59	5.62/3.03	
1b	355 (18 933), 425 (3285)	638	0.0020	0.54	579	0.12	16.1	2.51	5.55/3.04	
2a	387 (18 972)	596	0.0035	5.20	559	0.12	53.8	2.69	5.62/2.93	
2b	383 (18 671)	612	0.015	1.92	564	0.16	33.8	2.67	5.55/2.88	

^a Error $\pm 10\%$. ^b Fitted by single-exponential. ^c Since the decay is best-fit by double-exponentials, a weighted-average lifetime (τ_{ave}) was used and calculated by the equation $\tau_{ave} = \sum(A_i \tau_i / \sum A_i)$, where A_i is the pre-exponential for the lifetime τ_i . ^d Calculated from the absorption edge. ^e Estimated by cyclic voltammetry in dichloromethane with ferrocene (4.8 eV) as the reference. ^f Derived from the relation, $\Delta E = HOMO - LUMO$.

strongly depend on the rigidity of the medium, which is often observed in well defined MLCT Cu^I complexes.^{2a,2c,11} We speculate that the MLCT bands disappear in the absorption spectra of the neutral complexes can be explained in terms of that the MLCT bands blue shift and superimpose on the red shifted $\pi-\pi^*$ band. Therefore the lowest excited state of the neutral complexes may be attributed to the MLCT plus LC (ligand-centered $\pi-\pi^*$ transition) state. Generally, for those Ir^{III} or Os^{II} phosphorescent complexes dominated by a mixed state involving both MLCT and LC character, the larger extent of the LC character will blue shift their emission spectra as well as prolong their lifetimes (or decrease k_r).¹⁴ The relatively longer lifetimes and blue-shifted emissions observed in neutral complexes **2a** and **2b** further confirm that the lowest energy excited state of these neutral Cu^I complexes should contain a proportion of LC character.

For comparison to the cationic Cu^I complexes, the corresponding neutral one exhibits a larger HOMO–LUMO gap (Table 2) and a higher energy emission. In order to find out which orbital, HOMO or LUMO, increases the MLCT energy gap, the electrochemical properties of the four complexes were investigated by cyclic voltammetry at room temperature in dried and argon purged CH₂Cl₂ solutions. As revealed by the data in Table 2, each pair of complexes have the same HOMO energy level calculated from the oxidation potential onset, -5.62 eV for **1a** and **2a**, -5.55 eV for **1b** and **2b**, respectively. These results suggest that the negative charge in qbm ligand pushes up the energy level of LUMO, leading to a larger MLCT ($\pi^*(qbm) \leftarrow d^{10}(Cu)$) energy and a higher energy emission.

Electroluminescence

By spin-coating the emitting layer, multilayer OLEDs with the configuration of ITO/PEDOT/emitting layer (~ 50 nm)/BCP (20 nm)/Alq₃ (40 nm)/LiF (1 nm)/Al (~ 100 nm) were fabricated to evaluate the electrophosphorescent properties of the cuprous complexes, as shown in Fig. 7. In this configuration, BCP (2,9-dimethyl-4,7-diphenyl-1,10-phenanthroline) and Alq₃ [tris(8-hydroxyquinolato) aluminium] act as the exciton blocking and electron transporting materials, respectively.

Similar to those [Cu(NN)(PP)]⁺ systems,^{2a,2c} the electroluminescent (EL) spectra of **1b** or **2b** are identical to photoluminescent (PL) ones in PMMA film. Fig. 8 shows PL spectra and EL spectra of **1b** and **2b** in TCCz host as examples. In contrast to the PL spectra, no emission from the host was found in EL spectra, indicating that charge trap occurred in the device operation beside the energy-transfer process.^{2c}

The data of OLEDs performance are listed in Table 3. Although the PL quantum yield of **1a/1b** or **2a/2b** in PMMA is almost the same, the devices based on **1a** and **2a** exhibit much poorer EL performance. This may be associated with their poorer thermal stability (as revealed by thermal gravimetric analysis) and the ligand exchange reaction in solution during fabricating device with mono-dentate ligand PPh₃.^{1,2} With a doping concentration of 10 wt% in TCCz, device with a turn-on voltage of 7.5 V, maximum current efficiency of 5.58 cd A⁻¹, maximum brightness of 2820 cd m⁻² has been realized for **1b**.

As for the neutral Cu^I complex **2b**, devices with different doping concentrations varying from 2, 5, 10 and 20 wt% were fabricated

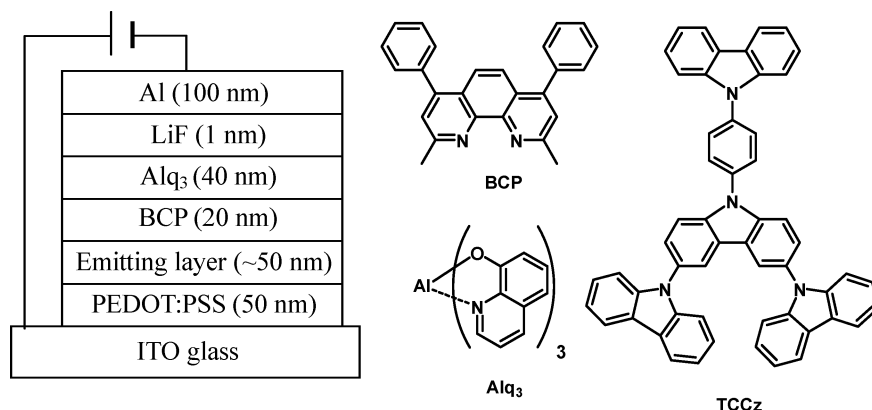
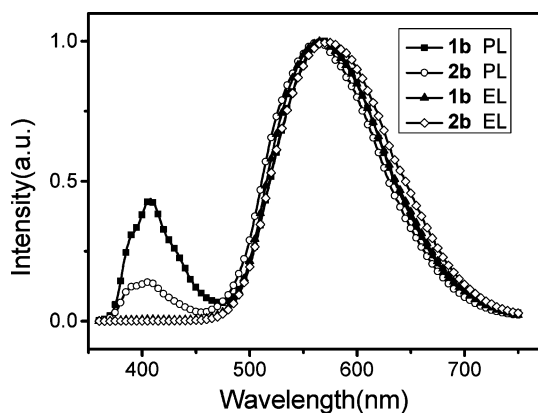


Fig. 7 The device architecture (left) and the molecular structures of the relevant compounds (right).

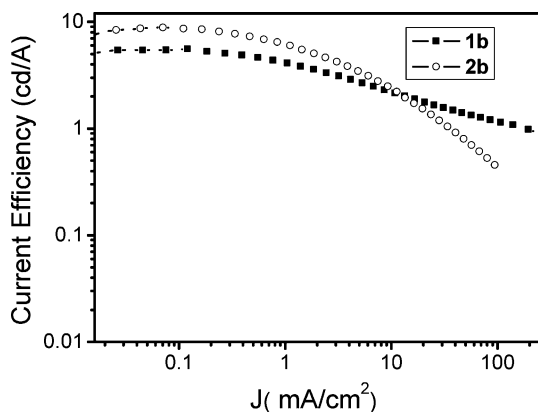
Table 3 Turn-on voltage (V_T), current efficiency (η_c), maximum brightness (B_{max}), emission wavelength (λ_{max}) of the OLEDs based on Cu^I complexes

Emitting layer	D C (wt%)	V_T/V	$\eta_{c,max}/cd A^{-1}$	$\eta_c^a/cd A^{-1}$	$\eta_c^b/cd A^{-1}$	$B_{max}/cd m^{-2}$	λ_{max}/nm
1a	10	11.9	1.39	1.32	0.88	885	571
2a	10	15.1	0.46	0.35	0.14	20	547
1b	10	7.5	5.58	4.11	2.16	2820	562
2b	2	9.5	1.19	1.10	0.67	292	555
	5	9.1	3.89	2.40	0.98	210	564
	10	7.7	8.87	6.00	2.35	465	555
	20	9.7	3.68	2.32	0.96	260	555

^a Measured at $1 mA cm^{-2}$. ^b Measured at $10 mA cm^{-2}$.

**Fig. 8** Electroluminescence (EL) and photoluminescence (PL) spectra of **1b** and **2b** in TCCz.

to improve its electroluminescent property. As shown in Table 3, the current efficiencies of the devices increase to the highest with increasing the concentration to 10 wt%, and further enhancement of the concentration results in reduction of the current efficiency. Device with a turn-on voltage of 7.7 V, maximum current efficiency of $8.87 cd A^{-1}$, maximum brightness of $465 cd m^{-2}$ has been realized for **2b**. Furthermore, a noticeable finding is that below the current density of about $12 mA cm^{-2}$ (corresponding brightness of about $240 cd m^{-2}$), the current efficiency of device **2b** is higher than that of its counterpart **1b** at the doping concentration of 10 wt% (shown in Fig. 9). The lower efficiency of the devices of **1b** may be attributed to the increased current density, which was caused by the drifting and accumulating of BF_4^- counterions towards the anode (ITO) upon application of a bias.^{2a} In addition, the current efficiency of

**Fig. 9** The current density–efficiency plot of the device for **1b** and **2b**.

2b descends more sharply than **1b** at high current density since it exhibits longer decay lifetime thus tends to undergo triplet–triplet annihilation.¹⁶

Unfortunately, an attempt to fabricate multilayer phosphorescent OLEDs using the vacuum deposition technique is unsuccessful, though the thermolysis temperatures of neutral **1b** and **2b** are over $350 ^\circ C$. Decomposition of the neutral complexes, in company with the dissociation of the ligand proved by the presence of the ligand emissive peak, was observed during the alone subliming, indicating their poor volatility due to their high formula weight. Therefore, synthesis of fluorinated⁵ or similar neutral Cu^I complexes⁶ that exhibit increased volatility should be desirable for deposited OLEDs.

Conclusion

In summary, this paper describes the dramatic emission properties of neutral mononuclear Cu^I complexes relative to the corresponding cationic complexes. These compounds can act as models for understanding the relationship between structural factors and photophysical properties due to their completely identical skeletons. The increased aromaticity and the decreased electron accepting ability of the negatively charged NN ligand result in a blue-shift emission from MLCT plus LC excited state in neutral Cu^I complexes. The results obtained from the study of PL and EL have demonstrated that the neutral Cu^I complexes possess similar luminescent performance to ionic ones and are a kind of more effective phosphorescent emitter for OLEDs.

Experimental

General

All experiments were carried out without special treatments. $[Cu(CH_3CN)_4](BF_4)$ ¹⁷ and 2-(2-quinolyl)benzimidazole (Hqbm)¹⁸ were prepared by literature procedures. Triphenylphosphine (PPh_3) and bis(2-diphenylphosphinophenyl)ether (DPEphos) were purchased from Aldrich Chemical Co.

Characterization. 1H NMR spectra with tetramethylsilane (TMS) as internal reference and ^{31}P NMR spectra with 85% H_3PO_4 as external reference were recorded on a Bruker Avance 300 NMR instrument. The film samples for photophysical studies were prepared by spin-coating a mixture of Cu^I complex (20 wt%) and poly(methyl methacrylate) (80 wt%) in methylene chloride onto a glass slide. UV-vis absorption and photoluminescence spectra were recorded by a Perkin-Elmer Lambda 35 UV/VIS

spectrophotometer and a HORIBA Jobin-Yvon FluoroMax-4 spectrometer, respectively. The solution PL quantum yield was measured with $[\text{Ru}(\text{bpy})_3]^{2+}$ as the reference in degassed water.¹⁹ The film PL quantum yield and the lifetime of both solution and film were measured according to the method reported previously.¹¹ Thermal gravimetric analysis (TGA) was carried out using the Perkin-Elmer-DSC7 instrument under a nitrogen atmosphere at a heating rate of $20\text{ }^\circ\text{C min}^{-1}$. Elemental analyses (C, H and N) were determined using a Bio-Rad elemental analysis system. Cyclic voltammetry were performed on an EG&G 283 (Princeton Applied Research) potentiostat/galvanostat system at room temperature with a conventional three-electrode system consisting of a platinum working electrode, a platinum counter electrode and an Ag/AgCl reference electrode. The measurements were carried out in dried and argon purged CH_2Cl_2 solutions with 1.0 mM of Cu^I complexes at a scan rate of 0.1 V s^{-1} . The supporting electrolyte was 0.1 M of *n*-tetrabutylammonium hexafluorophosphate (TBAH). The potentials are quoted against the ferrocene internal standard. The $\text{p}K_a$ values were measured using spectra methods with $\text{KH}_2\text{PO}_4/\text{KCl}$ as buffer solution in 6:4 methanol–water (v/v) at $25\text{ }^\circ\text{C}$.

X-Ray crystallography†. The crystals of the complexes were obtained *via* a solution-diffusion method. All diffraction intensities were collected at 186 K on a Bruker Smart APEX CCD area-detector diffractometer (MoK α , $\lambda = 0.71073\text{ \AA}$). The crystal structure was solved using the SHELXTL program and refined using full matrix least squares.²⁰ The hydrogen atom positions were calculated theoretically and included in the final cycles of refinement in a riding model along with attached carbon atoms.

Devices fabrication and characterization. To fabricate OLEDs, a 50 nm thick poly(ethylenedioxythiophene)/poly(styrene sulfonic acid) (PEDOT : PSS, purchased from H.C. Starck) film was first deposited on the pre-cleaned ITO-glass substrates with a sheet resistance of $100\text{ }\Omega/\text{square}$ and then cured at $120\text{ }^\circ\text{C}$ in air for 30 min. Then the emitting layer was prepared by spin-coating a dichloromethane solution of a mixture of the host material and the cuprous complexes [TCCz: $\text{Cu}^I = 10:1$ wt.] at a concentration of 6.0 mg mL^{-1} , respectively, forming a film around 50 nm. Successively, 20 nm of BCP, 40 nm of Alq_3 , 1 nm of LiF and 100 nm of Al were evaporated at a base pressure less than 10^{-6} Torr (1 Torr = 133.32 Pa) through a shadow mask with an array of 9 mm^2 opening. The electroluminescence (EL) spectra were recorded on a Horiba Jobin-Yvon FluoroMax-4 spectrometer. The current–voltage and brightness–voltage curves of the devices were recorded on a Keithley 2400/2000 source meter and a calibrated silicon photodiode. All measurements on the devices were carried out at room temperature under ambient conditions.

Synthesis

[Cu(Hqbm)(PPh₃)₂](BF₄) (1a). A dichloromethane solution (10 ml) of $[\text{Cu}(\text{CH}_3\text{CN})_4](\text{BF}_4)$ (0.314 g, 1.0 mmol), PPh₃ (0.525 g, 2.0 mmol) and Hqbm (0.245 g, 1.0 mmol) was stirred at room temperature for 5 h to give an orange solution. The solution was then filtered and evaporated to dryness. The residue was dissolved in dichloromethane and diffusion of methanol vapor into its concentrated solution gave orange crystals of **1a** (0.77 g, 84%).

TGA $277.2\text{ }^\circ\text{C}$. Anal. Calcd. for $\text{C}_{52}\text{H}_{41}\text{BCuF}_4\text{N}_3\text{P}_2$: C, 67.9; H, 4.5; N, 4.6%. Found: C, 67.8; H, 4.1; N, 4.5%. ¹H NMR (CDCl_3 , 300 MHz): δ 12.72 (s, 1H), 8.64 (d, 1H, $J = 8.58\text{ Hz}$), 8.52 (d, 1H, $J = 8.58\text{ Hz}$), 8.00 (d, 1H, $J = 8.19\text{ Hz}$), 7.93 (t, 2H, $J = 8.37\text{ Hz}$), 7.56 (t, 1H, $J = 7.17\text{ Hz}$), 7.38–7.28 (m, 9H), 7.19–7.12 (m, 24H), 7.04 (d, 1H, $J = 8.22\text{ Hz}$). ³¹P NMR: -1.10 (s). $\text{p}K_a$, 9.47 ($25\text{ }^\circ\text{C}$, in 6:4 methanol–water).

[Cu(Hqbm)(DPEphos)](BF₄) (1b). A dichloromethane solution (10 ml) of $[\text{Cu}(\text{CH}_3\text{CN})_4](\text{BF}_4)$ (0.314 g, 1.0 mmol), DPEphos (0.538 g, 1.0 mmol) and Hqbm (0.245 g, 1.0 mmol) was stirred at room temperature for 5 h to give an orange solution. The solution was then filtered and evaporated to dryness. The residue was dissolved in dichloromethane and diffusion of diethyl ether vapor into its concentrated solution gave orange crystals of **1b** (0.80 g, 86%).

TGA $355.6\text{ }^\circ\text{C}$. Anal. Calcd. for $\text{C}_{52}\text{H}_{39}\text{BCuF}_4\text{N}_3\text{OP}_2$: C, 66.9; H, 4.2; N, 4.5%. Found: C, 66.8; H, 4.0; N, 4.4%. ¹H NMR (CDCl_3 , 300 MHz): δ 12.19 (s, 1H), 8.43 (s, 2H), 7.99 (d, 1H, $J = 8.58\text{ Hz}$), 7.91 (d, 1H, $J = 7.92\text{ Hz}$), 7.80 (d, 1H, $J = 8.13\text{ Hz}$), 7.58 (d, 1H, $J = 8.16\text{ Hz}$), 7.47 (m, 1H), 7.40–7.16 (m, 9H), 7.13 (t, 6H, $J = 7.32\text{ Hz}$), 7.05 (t, 4H), 6.89 (m, 4H), 6.75 (t, 4H), 6.69 (dd, 4H). ³¹P NMR: -11.32 (s). $\text{p}K_a$, 9.11 ($25\text{ }^\circ\text{C}$, in 6:4 methanol–water).

Cu(qbm)(PPh₃)₂ (2a). A mixture of **1a** (0.230 g, 0.25 mmol) and KOH (0.20 g, 5 mmol) in methanol (100 ml) was stirred for 10 h at room temperature. After evaporating to dryness, the solid residue was extracted with dichloromethane. Subsequent diffusion of methanol vapor into its concentrated solution gave orange crystals of **2a** (0.17 g, 80%).

TGA $252.5\text{ }^\circ\text{C}$. Anal. Calcd. for $\text{C}_{52}\text{H}_{40}\text{CuN}_3\text{P}_2$: C, 75.0; H, 4.8; N, 5.1%. Found: C, 75.2; H, 4.6; N, 5.0%. ¹H NMR (CDCl_3 , 300 MHz): δ 8.71 (m, 1H), 8.21 (m, 1H), 7.86 (m, 1H), 7.77 (dd, 2H), 7.34–7.24 (m, 4H), 7.19–7.07 (m, 30H), 6.92 (br, 1H). ³¹P NMR: -1.07 (s).

Cu(qbm)(DPEphos) (2b). A mixture of **1b** (0.093 g, 0.10 mmol) and KOH (0.06 g, 1.5 mmol) in methanol (40 ml) was stirred for 12 h at room temperature. After evaporating to dryness, the solid residue was extracted with dichloromethane. Subsequent diffusion of diethyl ether vapor into its concentrated solution gave orange crystals of **2b** (0.05 g, 59%).

TGA $350.1\text{ }^\circ\text{C}$. Anal. Calcd. for $\text{C}_{52}\text{H}_{38}\text{CuN}_3\text{OP}_2$: C, 73.8; H, 4.5; N, 5.0%. Found: C, 73.8; H, 4.3; N, 4.8%. ¹H NMR (CDCl_3 , 300 MHz): δ 8.59 (d, 1H, $J = 8.55\text{ Hz}$), 8.18 (d, 1H, $J = 8.52\text{ Hz}$), 7.87 (t, 2H, $J = 8.49\text{ Hz}$), 7.69 (t, 2H, $J = 8.49\text{ Hz}$), 7.49 (m, 4H), 7.26–6.74 (m, 30H). ³¹P NMR: -13.43 (s).

Acknowledgements

This work is supported by the National Natural Science Foundation of China (No. 20874098 and 50673088), the Natural Science Foundation of Fujian Province (No. 2007F3116), Science Fund for Creative Research Groups (No. 20621401) and 973 Project (2009CB623600).

References

- (a) N. Armaroli, G. Accorsi, F. Cardinali and A. Listorti, *Top. Curr. Chem.*, 2007, **280**, 69; (b) A. Barbieri, G. Accorsi and N. Armaroli, *Chem. Commun.*, 2008, 2185.
- (a) Q. Zhang, Q. Zhou, Y. Cheng, L. Wang, D. Ma, X. Jing and F. Wang, *Adv. Mater.*, 2004, **16**, 432; (b) Q. Zhang, Q. Zhou, Y. Cheng, L. Wang, D. Ma, X. Jing and F. Wang, *Adv. Funct. Mater.*, 2006, **16**, 1203; (c) Q. Zhang, J. Ding, Y. Cheng, L. Wang, Z. Xie, X. Jing and F. Wang, *Adv. Funct. Mater.*, 2007, **17**, 2983; (d) N. Armaroli, G. Accorsi, M. Holler, O. Moudam, J.-F. Nierengarten, Z. Zhou, R. T. Wegh and R. Welter, *Adv. Mater.*, 2006, **18**, 1313; (e) G. Che, Z. Su, W. Li, B. Chu and M. Li, *Appl. Phys. Lett.*, 2006, **89**, 103511.
- P.-T. Chou and Y. Chi, *Eur. J. Inorg. Chem.*, 2006, 3319.
- Q. Zhang, Ph.D. Dissertation, Changchun Institute of Applied Chemistry, Chinese Academy of Sciences, 2005.
- H. V. Rasika Dias, H. V. K. Diyabalanage, M. A. Rawashdeh-Omary, M. A. Franzman and M. A. Omary, *J. Am. Chem. Soc.*, 2003, **125**, 12072; H. V. Rasika Dias, H. V. K. Diyabalanage, M. G. Eldabaja, O. Elbjeirami, M. A. Rawashdeh-Omary and M. A. Omary, *J. Am. Chem. Soc.*, 2005, **127**, 7489.
- (a) S. B. Harkins and J. C. Peters, *J. Am. Chem. Soc.*, 2005, **127**, 2030; (b) J. C. Deaton, S. C. Switalski, D. Y. Kondakov, R. H. Young, T. D. Pawlik, D. J. Giesen, S. B. Harkins, A. J. M. Miller, S. F. Mickenberg and J. C. Peters, *J. Am. Chem. Soc.*, 2010, **132**, 9499.
- A. J. M. Miller, J. L. Dempsey and J. C. Peters, *Inorg. Chem.*, 2007, **46**, 7244.
- N. Armaroli, G. Accorsi, G. Bergamini, P. Ceroni, M. Holler, O. Moudam, C. Duhayon, B. Delavaux-Nicot and J. F. Nierengarten, *Inorg. Chim. Acta*, 2007, **360**, 1032.
- P. C. Alford, M. J. Cook, A. P. Lewis, G. S. G. McAuliffe, V. Skarda, A. J. Thomson, J. L. Glasper and D. J. Robbins, *J. Chem. Soc., Perkin Trans. 2*, 1985, 705.
- R. D. Costa, E. Ortí, H. J. Bolink, S. Graber, S. Schaffner, M. Neuburger, C. E. Housecroft and E. C. Constable, *Adv. Funct. Mater.*, 2009, **19**, 3456.
- L. Qin, Q. Zhang, W. Sun, J. Wang, C. Lu, Y. Cheng and L. Wang, *Dalton Trans.*, 2009, 9388.
- S.-M. Kuang, D. G. Cuttall, D. R. McMillin, P. E. Fanwick and R. A. Walton, *Inorg. Chem.*, 2002, **41**, 3313.
- T. M^cCormick, W.-L. Jia and S. Wang, *Inorg. Chem.*, 2006, **45**, 147.
- (a) L. He, J. Qiao, L. Duan, G. Dong, D. Zhang, L. Wang and Y. Qiu, *Adv. Funct. Mater.*, 2009, **19**, 2950; (b) Y.-L. Chen, S.-W. Li, Y. Chi, Y.-M. Cheng, S.-C. Pu, Y.-S. Yeh and P.-T. Chou, *ChemPhysChem*, 2005, **6**, 2012; (c) Y.-M. Cheng, G.-H. Lee, P.-Tai Chou, L.-S. Chen, Y. Chi, C.-H. Yang, Y.-H. Song, S.-Y. Chang, P.-I. Shih and C.-F. Shu, *Adv. Funct. Mater.*, 2008, **18**, 183.
- (a) J. Pommerehne, H. Vestweber, W. Guss, R. F. Mahrt, H. Bassler, M. Porch and J. Daub, *Adv. Mater.*, 1995, **7**, 551; (b) M. Thelakkat and H. W. Schmidt, *Adv. Mater.*, 1998, **10**, 219.
- M. A. Baldo, C. Adachi and S. R. Forrest, *Phys. Rev. B: Condens. Matter Mater. Phys.*, 2000, **62**, 10967.
- G. J. Kubas, *Inorg. Synth.*, 1979, **19**, 90.
- T. Hisano, M. Ichikawa and K. Tsumoto, *Chem. Pharm. Bull.*, 1982, **30**, 2996.
- J. Van Houten and R. J. Watts, *J. Am. Chem. Soc.*, 1976, **98**, 4853.
- G. M. Sheldrick, *SHELXTL*, version 5.1, Bruker Analytical X-ray Systems, Inc., Madison, WI 1997.